Rheology at the Phase Transition Boundary: 1. Lamellar L_α Phase of AOT Surfactant Solution

P. G. Petrov,† S. V. Ahir,‡ and E. M. Terentjev*

Cavendish Laboratory, University of Cambridge, Madingley Road, Cambridge CB3 0HE, United Kingdom

Received April 1, 2002. In Final Form: June 17, 2002

The phase behavior of the binary mixture of an anionic surfactant Aerosol OT (AOT) and glycerol (used as a model for water) is investigated using rheological, optical, and X-ray synchrotron techniques. In particular, the storage shear modulus G' response, as a function of temperature and strain amplitude, has been related to the structural transformation into the lamellar L_α phase surfactant bilayers. Results demonstrate a characteristic critical behavior at the phase transition boundary $T = T_c$. Stress−strain variation indicates the shear-induced alignment of the layer system with a universal scaling of stress−strain.

1. Introduction

Complex fluid systems such as surfactant/water combinations have been intensely and systematically studied for many years. Industrially, surfactant products,[1] such as detergents and emulsions, continually experience varied and sometimes unpredictable shear regimes; despite a number of great advances, we are still unable to command their full understanding. Beyond manufacturing interests, surfactant/water systems also have clear implications in the biology of cell membranes[2] and relating their structural and rheological properties may well lead to advances at the life science interface.

Above a certain critical concentration (critical micelle concentration, cmc), amphiphilic surfactant molecules aggregate in solution to form nanosized spherical micelles. Increasing the concentration leads to the formation of cylindrical micelles, which in turn order in hexagonally packed arrays. Progressing further along the increasing surfactant concentration on a typical phase diagram, one sometimes finds a narrow region of bicontinuous cubic (and sponge) phases and finally arrives at the region of lamellar order, when surfactant is aggregated in flat bilayers, which are stacked in an essentially one-dimensional periodic lattice. On further reducing the proportion of solvent, one frequently finds the same sequence of inverted phases: see, for instance, refs 3−5. All anisotropic phases, possessing differing degrees of partial translational and orientational order, have a generic name of lyotropic liquid crystals.

One of the most typical (and most studied) ionic surfactants producing a broad lamellar phase is Aerosol OT (AOT). Some classical papers of the past report on the fundamental properties of phases in AOT/water systems,[6−8] but the original references to the studies of AOT go much further back. The phase diagram of the binary system of AOT/water is thought to be well established, Figure 1a, exhibiting a broad lamellar phase (with a two-phase region outside the spinodal), a narrow region of bicontinuous cubic phase at ∼80% AOT, and an inverse hexagonal phase at higher concentrations. At high temperatures, above the lamellar phase, one finds the isotropic liquid, which has to be interpreted as a solution of spherical micelles with a volume fraction corresponding to the given proportion of AOT in the system. Figure 1b shows the reported phase diagram for the AOT−glycerol system. Chemically, glycerol is very similar to water, but the relative weight of hydrophobic interactions is much reduced, which results in much lower temperatures of isotropic−lamellar transition.

In this paper, we examine the rheology of a lyotropic liquid crystal phase as it emerges during the phase transformation. Important efforts in studying the rheology of lamellar phases were made by Robles-Vasquez et al.,[9] Müller et al.,[10] Meyer et al.,[11] and others. However, a gap still remains in our understanding of material behavior in and around the phase transition region. The wide commercial availability of AOT and the ease with which the lamellar phase can be isolated make it an obvious choice upon which to experiment.

Though this paper briefly addresses the lamellar ordering and shear-induced alignment (for which Müller et al.[10] and many other authors[12,13] have accounted well), it more importantly demonstrates rheological results as

* To whom correspondence should be addressed. E-mail: emt1000@cam.ac.uk.

† Present address: Department of Physics, University of Exeter, EX4 4QL.

‡ Present address: Imperial College of Science, Technology and Medicine, London SW7 2AY.

(1) Terry, A. E.; Odell, J. A.; Nicol, R. J.; Tiddy, G. J. T.; Wilson, J. E. *J. Phys. Chem. B* **1999**, *103*, 11218.

(2) Israelachvili, J. *Intermolecular and Surface Forces*; Academic Press: London, 1992.

(3) Tiddy, G. J. T. *Phys. Rep.* **1980**, *57*, 1.

(4) Laughlin, R. G. *The Aqueous Phase Behaviour of Surfactants*; Academic Press: London, 1994.

(5) Fredrickson, G. H.; Bates, F. S. *Annu. Rev. Mater. Sci.* **1996**, *26*, 501.

(6) Rogers, J.; Winsor, P. A. *J. Colloid Interface Sci.* **1969**, *30*, 247.

(7) Strey, R.; Jahn, W.; Skouri, M.; Porte, G.; Marignan, J.; Olsson, U. In *Structure and Dynamics of Strongly Interacting Colloids and Supramolecular Aggregates in Solutiuon*; Kluwer Academic: Dordrecht, 1992.

(8) Fontell, K. In *Colloid Dispersions and Micellar Behavior*; ACS Symposium Series Vol. 9; American Chemical Society: Washington, DC, 1975; p 270.

(9) Robles-Vasquez, O.; Corona-Galván, S.; Soltero, J. F. A.; Puig, J. E.; Tripodi, S. B.; Vallés, E.; Mannero, O. *J. Colloid Interface Sci.* **1993**, *160*, 65.

(10) Müller, S.; Börschig, C.; Gronski, W.; Schmidt, C. *Langmuir* **1999**, *15*, 7558.

(11) Meyer, C.; Asnacios, S.; Bourgaux, C.; Kleman, M. *Rheol. Acta* **2000**, *39*, 223.

(12) Dhez, O.; Nallet, F.; Diat, O. *Europhys. Lett.* **2001**, *55*, 821.

(13) Imai, R.; Nakaya, K.; Kato, T. *Eur. Phys. J. E* **2001**, *5*, 391.

10.1021/la025792k CCC: $22.00
Published on Web 10/29/2002

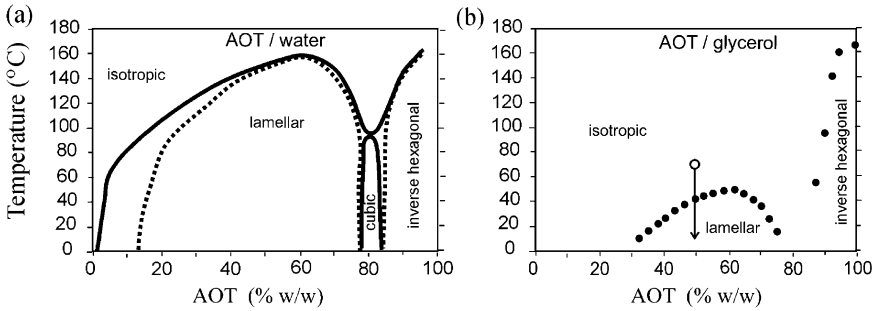

Figure 1. (a) The phase diagram of the AOT−water binary system, from ref 6. The main ordered phase is the lamellar L_α state, with a pocket of bicontinuous cubic and inverse hexagonal phases at high concentrations. (b) The phase diagram of the AOT−glycerol binary system, from ref 15, has similar features and topology, but with a much reduced isotropic−lamellar transition temperature. The arrow indicates the path through the phase boundary explored in this paper.

the sample follows different temperature profiles across the phase boundary. This aspect of the phase behavior is novel in itself, providing an additional dimension to the phase diagram, and can further be used to initiate an understanding of mechanisms taking place during the first-order phase transition between the isotropic mixture of spherical micelles and the lamellar packing of flat bilayers. Of course, there is a direct correspondence between the surfactant lamellar phase and that of microphase-separating block copolymers, which makes the topic of study even broader.

We are interested in the role the formation of lyotropic liquid crystal textures plays in the overall scheme of the mechanical behavior. In particular, the function of defects in the lamellar phase is of great interest. The effect of layer fluctuations and the increase of smectic order on cooling is also related to the result of shear rheology and structural study. The purpose of this work has been to investigate the effect of heating/cooling rates on the mechanical response (given by the storage shear modulus G') of a lamellar phase emerging at a transition temperature T_c. In addition, dynamic strain experiments are carried out at various temperatures to help develop the relationship between the stress and the strain amplitude, which is clearly nonlinear. These data describe the effect of shear alignment; we particularly focus on the relatively small shear rates, well below the celebrated onion states[14] and further high-shear regimes. Small-angle synchrotron X-ray experiments were also conducted to provide information about the layer spacing and the smectic order parameter, both affecting the layer compression constant B and, ultimately, the macroscopic shear modulus. Confocal microscopy provides additional information about the textures emerging at the phase transition and their evolution under shear.

For practical reasons, to be able to comfortably scan across the phase boundary, we use glycerol instead of water as the suspending matrix for AOT. As the phase diagrams in Figure 1 indicate, the topology of phase ordering should be the same in both systems (although, of course, the layer spacing is expected to change) but the transition temperature T_c is very much lower in glycerol, to allow an easy access to the isotropic liquid phase, which is not so straightforward for the AOT/water system. We expect the results to have a qualitative universality for all lyotropic lamellar materials.

2. Experimental Section

Materials. The anionic surfactant AOT, sodium salt of bis-(2-ethylhexyl)sulfosuccinate, is a widely available commercial product; our batch, with a purity greater than 99%, was obtained from Aldrich Chemicals. The molecule of AOT has two branched hydrophobic tails, which promotes flat layers with low spontaneous curvature on aggregation, and thus the dominant lamellar phase. For the AOT/water binary system, we used distilled and deionized water, the conditions we expect to be reproduced in the AOT/glycerol system. Glycerol ($CH_2OH-CHOH-CH_2OH$, 99% purity, from BDH Chemicals) has similar hydrogen-bonding properties as H_2O but much higher viscosity and lower evaporation temperature. One accordingly expects[15] to find very similar phase behavior on mixing it with ionic surfactants.

Glycerol was added at room temperature to dried AOT (at a fixed proportion of 50 wt % AOT, 50 wt % glycerol). The batch was then mixed by a IKAMAG RCT magnetic stirrer for several hours, set at 60 Hz and 70 °C, and then stored for several days at 70 °C. To ensure full mixing and homogeneity throughout the sample, we also subjected the batch to ultrasound excitation for an hour every day for about a week. This formed the desired material with a homogeneously mixed AOT/glycerol at high temperatures and the well-defined lamellar L_α phase below 45 °C. Although there might have been an issue of AOT hydrolysis in glycerol (cf. ref 16), we have been able to confirm that all rheological results and the thermal signature of the phase transition were reproducible for many weeks after the sample preparation.

The structure and properties of the lamellar L_α phase of AOT systems are known to strongly depend on the concentration of salt in solution; see for example ref 7. This is expected, as the ionic surfactant provides a lot of electrostatic interaction and its screening would have a vital effect. To narrow the range of possible variables in the problem, we work with the salt-free solutions, a truly binary AOT/glycerol system.

Rheometry. Rheological measurements were staged on a stress-controlled Rheometrics DSR (dynamic stress rheometer) connected to a water bath heater, an acceptable source for our temperature range between 5 and 70 °C. A cone and plate geometry (25 mm, 0.1 rad) was used as clearly this ensures a consistent shear rate in the total volume of the liquid.[17] An added precaution was to keep the distance between the cone tip and the bottom plate relatively small at 55 ± 5 μm ensuring that a homogeneous shear stress was experienced throughout the sample. Finally, the sample perimeter was carefully coated with low-viscosity silicone oil to prevent atmospheric moisture absorption.

The main batch of sample was contained in an airtight bottle, and specimens to be tested were removed after melting and homogenization of the sample. Once melted, the samples were loaded into the rheometer without allowing them to cool below T_c. The thermal and stress history can have a profound effect on lyotropic liquid crystal phases. To ensure that no such history was recorded in the material, all samples have been presheared to instate a uniform starting condition. Therefore, all tests were carried out using fresh samples from the same batch, which were thermally equilibrated for 30 min in the isotropic phase at 60 °C and then presheared with a stress of 10 Pa.

(14) Diat, O.; Roux, D.; Nallet, F. *J. Phys. II* **1993**, *3*, 1427.

(15) Nees, D.; Wolff, T. *Langmuir* **1996**, *12*, 4960.
(16) Sager, W. F. C. *Langmuir* **1998**, *14*, 6385.
(17) Léon, A.; Bonn, D.; Meunier, J.; Al-Kahwaji, A.; Kellay, H. *Phys. Rev. Lett.* **2001**, *86*, 938.

The first series of rheological experiments involved observing the onset and evolution of the lamellar phase as the sample was cooled and heated at different rates. Measurements were performed under low-amplitude oscillatory shear, at a relatively low frequency of 1 Hz, with an initial applied stress of 1 Pa. Samples were presheared at 60 °C, cooled to around 15 °C at various rates, and then heated back up to 60 °C. The variation of the storage modulus (G') with temperature was examined throughout.

In these experiments, the main difficulty is to obtain a continuous signal when the system undergoes a rapid transition from a liquid to an essentially solid state, changing the effective shear modulus by many orders of magnitude. To achieve this, the strain amplitude was set using the rheometer control software to be automatically kept between 1.25 and 1.5%. Maintaining the strain amplitude on a stress-controlled rheometer requires the automatic stress adjustment. This adjustment is achieved by a stepwise increment of the torque applied to the shear cell, until the returned measured strain achieves its target value.

The second series of rheological experiments required direct observation of the variation of G' with strain amplitude for the lamellar material. Again, the samples were presheared at relatively high temperatures and then cooled slowly to the testing temperature. Once equilibrated, a constant static force is applied (at a constant frequency of 1 Hz) to provide a strain increase in intervals of 1% up to 50% and the G' response is recorded.

X-ray Diffraction. Small-angle X-ray diffraction (SAXS) studies were performed at station 8.2 of the synchrotron radiation source at Daresbury Laboratory, Cheshire, U.K. The small angle detector camera length was set between 1.5 and 3.5 m, thus providing the scattering vector values in the range of 0.05−0.30 $Å^{-1}$. Samples were held between a mica sheet of 0.1 mm and an aluminum plate (mica supplied by Goodfellow, Cambridge, U.K.), with a brass spacer of 0.25 mm thickness. The metal substrate plate was used to ensure accurate heat transfer to and from the sample. Sample temperature was controlled by a Lauda water-bath and verified by the Linkam TP91 hot stage. Three different samples from the same batch (50 wt % AOT/glycerol) were tested using the setup mentioned above, providing the matching data for the lamellar spacing, d.

Differential Scanning Calorimetry (DSC). A Perkin-Elmer power-compensated Pyris 1 differential scanning calorimeter was used for all experiments. To focus on the isotropic−lamellar transition, samples were held at 70 °C for 15 min, cooled to 30 °C at a specified rate, held for 15 min, and then reheated to 55 °C at the same rate. The experiment was then repeated at a different temperature rate with the same sample, and transition temperatures were extrapolated to the zero cooling rate, which was perceived as the equilibrium value.

Shear Stage Confocal Microscopy. A Zeiss LSM 510 confocal microscope was used to provide more three-dimensional images of the binary system. A Linkam shear stage CSS450 device was also attached in an attempt to reproduce the conditions set up in the rheological study. Samples were sheared at 10 Pa while in the isotropic liquid phase (around 60 °C) to remove any stress history. They were then cooled with pictures being taken from 45 °C at 30 s intervals until the lamellar phase was well established at room temperature. The cooling rate was not accurately controlled due to the limitations of the shear stage equipment, and thus the samples were cooled at an ambient rate. During the cooling cycle, a strain amplitude was maintained at 1.5% at a frequency of 1 Hz.

3. Structural Transformation

Phase Transition and Textures. The phase diagram of the binary AOT/water system is well established. However, in the case of glycerol substitution for water and in light of recent more sensitive techniques, it was of interest to revisit the isotropic−lamellar phase transition region in this system. Establishing the point at which phase transition occurs at a given concentration is of paramount importance. To this end, DSC traces are made with the latent heat peaks shown in Figure 2. The width

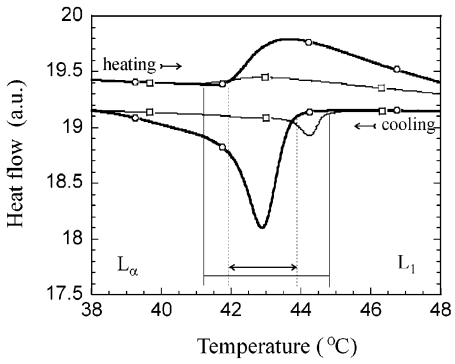

Figure 2. Heating and cooling DSC scans of the 50 wt % AOT/glycerol binary system, obtained at rates of 5 °C/min (circles) and 1 °C/min (squares). The width of the two-phase region between the isotropic and the lamellar phase is marked by vertical lines (the width decreases with a higher rate of temperature change).

of the two-phase region separating the phases decreases when the rate of cooling or heating increases, an expected result, common to phase-separating mixtures.

The two-phase transition region and the low-temperature L_α phase are visually confirmed by both confocal and optical microscopy. As the confocal images in Figure 3 demonstrate, the characteristic focal conic texture forms below the transition region, as expected of smectic phases.[18] The texture forms on cooling by nucleation and growth; however, when the system is held at 43 °C (in the middle of the transition region) the two-phase state remains stable, with lamellar regions (with focal conics) separating the regions of isotropic fluid, Figure 3a. The presence of the two-phase zone provides a viable explanation to some of the rheological data discussed below. No further discussion of the microscopy and textures is given here; we mention only that the faster cooling rate results in more nucleating structures and hence the smaller size of the texture domains. This is also of some significance later.

Lamellar Spacing and Fluctuations. Synchrotron small-angle X-ray diffraction data on cooling the system from the isotropic phase allow the accurate calculation of the lamellar spacing and a qualitative estimate of the smectic order parameter changing through a range of temperatures. As an illustration, Figure 4a shows the evolution of the diffraction peaks on cooling from 50 °C to below room temperature at a rate below 1 °C/min. It is clear that a broad peak exists above the transition temperature T_c, presumably reflecting the separation of spherical AOT micelles in the isotropic phase. Below T_c, the peak becomes much more narrow and its intensity grows rapidly, expressing the onset and saturation of lamellar ordering. Figure 4b gives more quantitative information about the scattering data. The d-spacing of the lamellar planes, estimated from the peak position in the reciprocal space as $d = 2\pi/Q_0$, provides the value $d \approx$ 36.4 Å at room temperature. These results are very reproducible for different samples of the same AOT/glycerol composition.

The characteristic length scale d grows rapidly before the transition from its value $d \approx 33.5$ Å at 50 °C. At 50 wt % concentration (accounting for the higher glycerol density, $\rho_{gl} \approx 1.22$ g/cm^3, giving the AOT volume fraction of ∼0.55), the geometrical calculation provides the mean separation of spherical micelles, $d \approx 1.15\times$ diameter.

(18) de Gennes, P. G.; Prost, J. *Physics of Liquid Crystals*; Clarendon Press: Oxford, 1993.

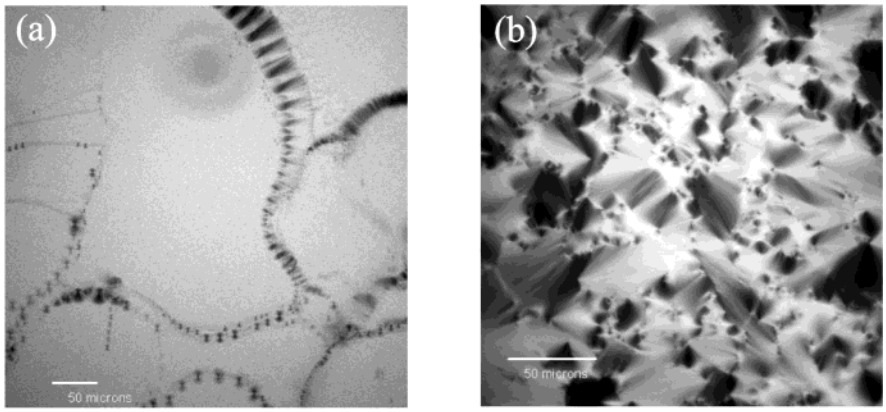

Figure 3. Microscopic textures of the 50 wt % AOT/glycerol binary system obtained with the confocal microscope, slicing through the texture ~100 μm below the top surface. The scale bar of 50 μm is shown on both images. The image in (a) is taken after temperature stabilization at 43 °C and shows the two-phase region with lamellar focal conic regions separating the regions of homogeneous isotropic phase. The room-temperature focal conic texture is shown in (b); importantly, this texture does not visibly change under the oscillating shear of $\dot{\epsilon} = 0.5\ s^{-1}$; see section 4.

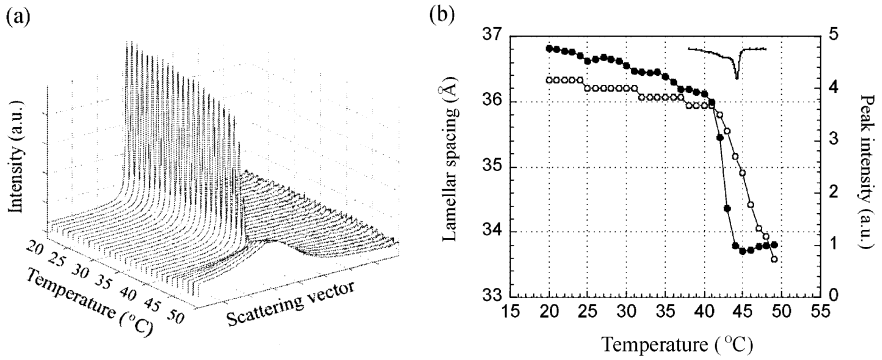

Figure 4. Small angle X-ray scattering results. (a) The evolution of structure on slow cooling from the isotropic phase. A small broad peak at Q_0 above $T_c \approx 45$ °C is an indication of spherical micellar aggregation; after the phase transition, the intensity of the reflection rapidly grows but hardly moves in the reciprocal space. (b) The lamellar spacing d (open circles, left y-axis) and the peak intensity (filled circles, right y-axis) as functions of temperature. The position of the corresponding DSC peak is also drawn for reference.

Taking $d \approx 33.5$ Å, we estimate the micelle diameter of 29 Å and, thus, the extended length of the AOT molecule of ~14.5 Å (this includes the size of the polar hydrophilic head and the counterion Stern layer). We feel that this value agrees well with the estimate of the extended length of the AOT hydrophobic tail, ~11 Å (this estimate is obtained directly from the Cerius[2] simulation package). Another similar estimate can be found in the literature and is based on the AOT molecular volume[19] of ~710 Å^3 and the area per molecule[20] of ~66 Å^2.

The lamellar spacing $d \approx 36$ Å is determined by the same estimate of the volume ratio at 50 wt % (1:1.22). In that case, the thickness of the glycerol layer separating the AOT lamellae is ~16 Å, while the bilayer thickness is ~20 Å. This again is very close to the doubled AOT length, although a small degree of tail interdigitation cannot be excluded. The fact that the lamellar spacing shows a slow increase on further cooling is puzzling, as one could expect a reduction in layer fluctuations and thus an increase in their density. The only reasonable explanation for this continuing increase in d is the increasing lateral compaction of AOT molecules inside the bilayer, leading to further straightening of the aliphatic tails and the effective increase in bilayer thickness.

The rapid growth of the peak intensity at $T = T_c$ is the expected signature of the increasing order at the first-order isotropic−lamellar phase transition. The intensity has a pronounced dip just above the T_c, which we interpret as the result of increased fluctuations (albeit noncritical) at the transition, when the assembly of relatively monodisperse spherical micelles transforms into a topologically very different lamellar structure. Below T_c, we find a continuing gradual increase in the scattering intensity. We associate this with the Debye−Waller factor reflecting the strength of thermal fluctuations in the lamellar phase and, thus, the value of the smectic order parameter $\psi(T)$. We shall see that the rheological response of the material follows the same trend, increasing the measured modulus at lower temperatures.

(19) Li, Z. X.; Lu, J. R.; Thomas, R. K. *Langmuir* **1997**, *13*, 3681.
(20) Fontell, K. *J. Colloid Interface Sci.* **1973**, *44*, 318.

4. Rheology at the Phase Boundary

Rheological experiments, central to this work, are conducted in two parts. The first series of tests involve observing the elastic storage modulus response as a function of temperature, at different cooling rates from the isotropic phase. This provides information about the phase transition and the reversible onset and further increase of order in the system. The second test focused on the variation of the response modulus with increasing amplitude of the oscillating strain (at fixed frequency and temperature), providing information about the onset of shear alignment in the lamellar phase.

Effect of Cooling Rate: Transition Kinetics. In this experimental protocol, the material is heated well into the isotropic phase and presheared to ensure the same

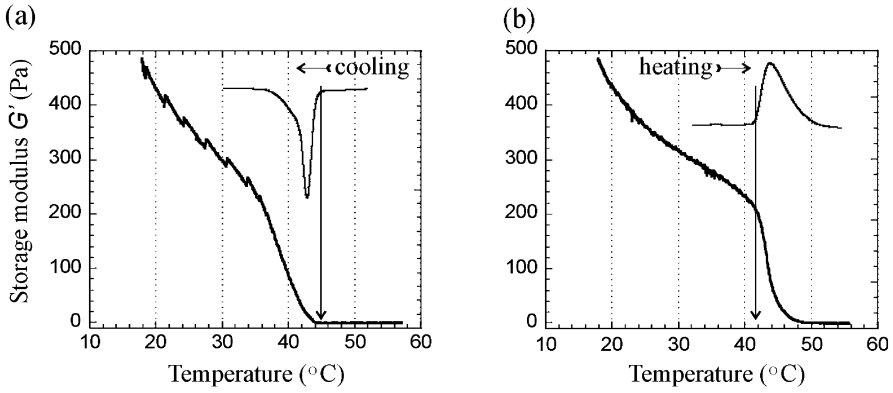

Figure 5. The reversible onset of mechanical stability (storage shear modulus G') on (a) cooling from the isotropic (L_1) to the lamellar L_α phase and (b) heating back to the isotropic phase, at a rate of 0.3 °C/min. Both plots show the corresponding thermal signature of the transition (DSC data, Figure 2) for reference.

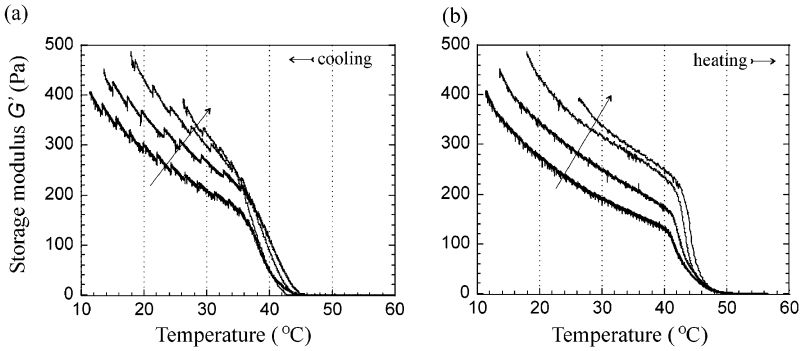

Figure 6. The evolution of storage modulus $G'(T)$, obtained at a frequency of 1 Hz and a strain amplitude of ~1.5%, for different cooling rates increasing from 0.01 to 0.09, 0.3, and 0.5 °C/min (in both plots the arrow indicates the increasing rates): (a) cooling from the isotropic liquid state; (b) heating to above T_c.

thermal and mechanical history of all samples. Then the sample is cooled through its phase transition zone at a specified and well-controlled temperature rate, maintaining the constant oscillating shear of amplitude 1.25−1.5% and the constant frequency of 1 Hz (that is, a low effective shear rate $\dot{\epsilon} = 0.0125-0.015\ s^{-1}$). A typical result is illustrated in Figure 5. The plots clearly show two regions: the rapid increase in mechanical rigidity, expressed by the storage shear modulus G' [the real part of the complex modulus $G^*(\omega)$] immediately below T_c and the gradual increase of G' with decreasing temperature. Comparing the plots on cooling and heating, one can conclude that the first region describes the two-phase system where the main contribution to the growth in G' is the increasing proportion of the elastic lamellar phase on cooling below T_c. A very similar observation has been recently made in ref 21 where a rapid growth in G' was registered in the two-phase region of a gelatin−maltodextrin solution.

Different cooling rates have been applied and provide two separate observations, summarized in Figure 6. First of all, as the cooling rate is increased, the onset of the two-phase lamellar region shifts to lower temperatures, as would be expected from the first-order phase transformation boundary. Similarly, on heating the onset of the two-phase region shifts to higher temperatures. Higher cooling rates result in a much higher level of elastic stability in the lamellar phase; we associate this with a smaller size of polydomain texture, resulting in a higher concentration of defects (dislocations and grain boundaries). In the next section, we shall study the shear alignment, when the increasing shear rate generates a more ordered system with fewer dislocations and grain boundaries and, as a result, with a lower overall G'. Defects strengthen the system by preventing an easy shear along the layer planes or their bending.

The increase in G' is achieved by an overall scaling (with some shifting along the T-axis due to supercooling). It appears that the underlying equilibrium temperature evolution is universal and matches the results of equilibrium structure studies by X-ray methods.

Effect of Strain Amplitude: Shear Alignment. For the second series of experiments, Figure 7a provides a useful illustration of the elastic response G' as the strain amplitude is increased for various temperatures. All samples studied in the series were cooled at the medium rate of ~0.3 °C/min from the presheared isotropic state to the particular temperature of observation. Accordingly, all samples have gone through the two-phase region and formed a polydomain lamellar phase with, crudely, the same concentration of defects, see Figure 3.

The obtained $G'(\epsilon)$ relationship clearly reflects the effect of shear alignment, discussed in the context of lamellar phases by many authors.[10−14] However, in contrast to most of the cited work and other reports in the literature, we examine the initial region of very small strain rates: at the constant frequency 1 Hz, $\dot{\epsilon}$ raises up to only 0.5 s^{-1} in Figure 7. At such a low level of imposed shear, one does not yet find any significant change in polydomain texture; the confocal microscopy image Figure 3b remains visually the same at $\dot{\epsilon} = 0.5\ s^{-1}$. At the same time, the drop in the mechanical modulus G' is very noticeable.

Moreover, although all curves in Figure 7a are obtained by increasing the strain amplitude, we also performed a

(21) Normand, V.; Pudney, P. D. A.; Aymard, P.; Norton, I. T. *J. Appl. Polym. Sci.* **2000**, *77*, 1465.

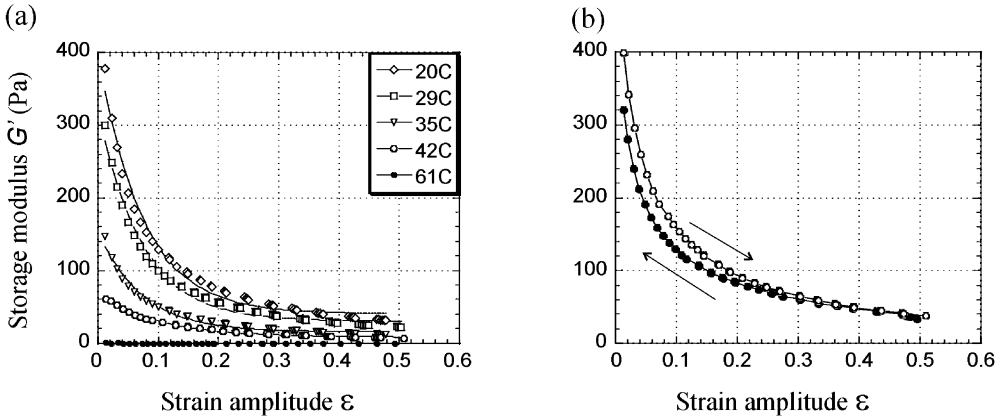

Figure 7. The effect of shear alignment is the reduction of effective storage modulus G'. (a) Raw data of $G'(\dot{\epsilon})$ at different temperatures (labeled on the plot). At 61 °C, the material is the isotropic liquid. Solid lines are fits by eq 1. (b) The mechanical response on increasing the strain amplitude and then decreasing it again, at a constant frequency of 1 Hz and $T = 17$ °C; see text. Despite a small hysteresis, the behavior is clearly reversible.

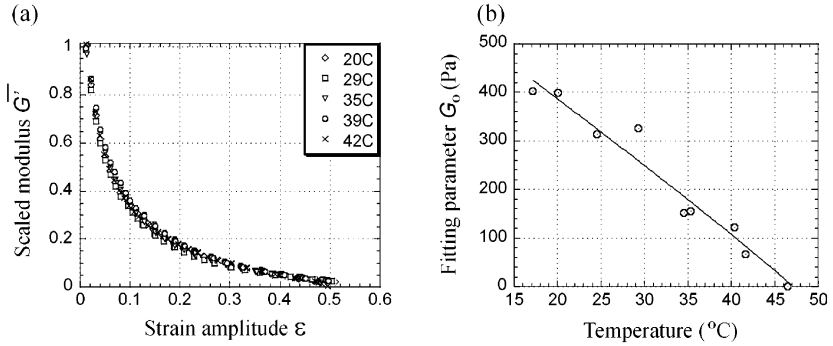

Figure 8. (a) The master curve for $\overline{G'}(\epsilon) = (G' - G_\infty)/(G_0 - G_\infty)$, obtained by scaling the data at all temperatures by the parameters of the model (eq 1); see text. (b) The fitting parameter G_0 for different temperatures of shear-aligning testing; the solid line shows the power-law fit $G_0 \propto |1 - T/T_c|^{0.93}$.

reverse experiment. One has to be careful not to overshear the material, when the texture changes become irreversible: we slowly increased ϵ to the level ~0.5 and then slowly reduced it back to zero (all at a fixed temperature). In this regime, the modulus G' increases again, with a very small hysteresis. This observation indicates that the initial regime of shear alignment occurs in a reversible way, when the network of defects in the material deforms in an "equilibrium" manner, Figure 7b. (At much higher strains, the lamellar texture would rearrange, and many observations of this can be found in the literature.)

The best fit of the data for $G'(\epsilon)$ at all temperatures below T_c is given by the simple exponential relation

$$G' = G_\infty + (G_0 - G_\infty)\mathrm{e}^{-\alpha\epsilon} \qquad (1)$$

which can, equally, be represented as $G'(\dot{\epsilon})$, the dependence on strain rate. Such a sharp variation with strain amplitude is rather unexpected. Evidently, two parameters of this fit are most essential: the equilibrium "linear response" value $G_0 = G'|_{\epsilon=0}$ and the exponent α. Both are, presumably, very strong functions of AOT concentration; however, at our fixed concentration we can examine only their trend with varying temperature. The exponent α obtained from the fits by eq 1 is remarkably constant: $\alpha = 0.12 \pm 0.01$, with no noticeable temperature variation at all. On the other hand, one expects the equilibrium modulus G_0 to be a function of temperature, through its dependence on the smectic order parameter. Figure 8 illustrates the details of the fitting analysis. According to the model, one can write the scaled modulus in the form

$$\overline{G'} = \frac{G'(\epsilon) - G_\infty}{G_0 - G_\infty} = \mathrm{e}^{-\alpha\epsilon}$$

The fact that all $G'(\epsilon)$ curves superpose in Figure 8a proves that the parameter α is indeed constant. Although the values of fitting parameter G_0 have some noise (the errors of fitting are smaller than the symbol size in Figure 8), there is also a clear trend in its temperature dependence. It is not unexpected: if we assume that the main contribution to the macroscopic modulus G' is due to the layer compression constant B (see a more full discussion below), which scales as the square of the smectic order parameter ($B \propto \psi^2$),[18] then the mean-field assumption of $\psi \propto |1 - T/T_c|^{1/2}$ is consistent with the data in Figure 8b.

However, at this stage it would be premature to assign any special significance to the success of the exponential model (eq 1). Although the constant value of α across a number of separate experiments is a comforting finding and the dependence $G_0(T)$ appears as a universal critical exponent, one must remember that we are dealing with the first-order phase transformation from the isotropic phase. Additional studies at different concentrations (thus crossing the phase boundary at a different point) should be performed before any firm theoretical conclusions are drawn.

In any case, we must also emphasize that the stress–strain response of the lamellar L_α phase of AOT is clearly nonlinear at all strain amplitudes we have examined. Even

at the lowest $\epsilon = 1.25\%$ (strain rate $\dot{\epsilon} \sim 10^{-2}$ s^{-1}), the modulus G' drops very sharply with increasing strain.

5. Conclusions

To the best of our knowledge, this is the first systematic study on emerging lamellar phase rheology during a first-order phase transition from a micellar solution. Although we used glycerol as a suspending medium, one may expect a similar rheological behavior with other (water-based) surfactant lamellar mesophases. We established a characteristic signature in the behavior of the storage modulus when the system is forced through the phase transformation: a fast change in mechanical rigidity close to the transition temperature (associated with the two-phase transition region) followed by a gradual increase of G' with decreasing temperature and the increase of the smectic order. This dependence of the layer compression modulus $B \sim \psi^2$ (one assumes that B also determines the macroscopic response modulus G' of the texture) has to be present regardless of the physical mechanism dominating the formation of the lamellar system: Helfrich interaction,[22] weak overlap at high screening,[2] or full electrostatic repulsion.[23] Accordingly, one expects a degree of universality of the results presented here for the particular system of AOT/glycerol.

The mechanical rigidity of the lamellar system can be controlled through the cooling rate and associated variation in the concentration of defects (dislocations and grain boundaries), whose main effect is to prevent the system from shear along the lamellae or their bending. This conclusion correlates well with direct evidence from optical microscopy revealing that faster cooling results in smaller domain size. Rheological scans of varying cooling/heating rates across the phase boundary could provide a very useful tool in studying the phase equilibrium and kinetics in ordered lyotropic systems.

Stress−strain experiments at a fixed temperature have also provided insight into the shear-induced alignment of polydomain lamellar structures at very low strain rates. Our results show an exponential decay of the storage modulus with the increasing strain amplitude at all temperatures below the lamellar transition, which leads us to speculate that the equilibrium linear response $G_0 \propto (1 - T/T_c)$ appears with a universal critical exponent of $\sim$1. Clearly, more experimental data are needed, at different compositions and for different lamellar systems, before generalizing such a conjecture. Importantly, in this initial regime of small strains (strain rates), the lamellar alignment is reversible: the reduction of shear amplitude returns the measured modulus to its high value characteristic of a polydomain system with a high concentration of defects.

Small-angle X-ray diffraction provides characteristic dimensions of the lamellar L_α phase (as well as the isotropic L_1 micellar solution). The trend of the storage modulus with temperature correlates very well with the structural data. Using this technique, we were able to monitor the change in lamellar spacing and the degree of smectic order with temperature. As expected, the intensity of the scattering peak increases for lower temperatures, signaling an increase in the smectic order parameter. Surprisingly, the lamellar spacing shows a slow increase on cooling deep into the lamellar phase, which suggests that the further compacting of the surfactant molecules is accompanied by straightening of the aliphatic tails.

In summary, this work provides a new, rheological dimension to the phase diagram of a complex fluid: ordered surfactant phases are mainly needed in technology because of their rheological properties and this was the motivation for our study.

Acknowledgment. We thank E. Kaler for helpful discussions. The help of J. Sanderson, in obtaining the SAXS X-ray data from the Daresbury synchrotron radiation source, and of I. Hopkinson and L. Kershaw, in confocal imaging, is gratefully appreciated. This work has been supported by EPSRC U.K.

LA025792K

(22) Helfrich, W. *Z. Naturforsch., A* **1977**, *33*, 305.
(23) Porcar, L.; Ligoure, C.; Marignan, J. *J. Phys. II* **1997**, *7*, 493.